*Engineering Fracture Mechanics* Vol. 21, No. 1, pp. 173–185, 1985
Printed in the U.S.A.

0013–7944/85 $3.00 + .00
Pergamon Press Ltd.

# FATIGUE CRACK GROWTH UNDER COMPRESSIVE LOADING

N. A. FLECK, C. S. SHIN and R. A. SMITH
Engineering Department, Cambridge University, Trumpington Street, Cambridge CB2 1PZ, England

**Abstract**—Fatigue cracks were grown in centre-notched sheet made from BS4360 50B structural steel. Despite the fact that loading was fully compressive, cracks initiated and grew in regions of residual tensile stress at the notch roots. It was observed that crack growth rates decreased with increasing crack length until arrest occurred. Near tip strain gauges were used to monitor crack closure; closure readings agreed well with those deduced from growth rates. The residual stress ahead of the slit tip and normal to the slit plane, $\sigma_{res}$, was estimated from the crack growth rate response. It was found that $\sigma_{res}$ scaled with distance, $x$, from the slit tip as $\sigma_{res} \alpha x^{-0.56}$.

## NOTATION

| | |
|---|---|
| $a$ | Semi-crack length, mm |
| $a_0$ | Initial semi-slit length, mm |
| $A$ | Strain hardening coefficient, MPa |
| $2b$ | Width of specimen; mm |
| $da/dN$ | Crack growth rate, mm/cycle |
| $E$ | Young's modulus, MPa |
| $K$ | Stress intensity, MPa$\sqrt{m}$ |
| $\Delta K$ | Nominal stress intensity range, MPa$\sqrt{m}$ |
| $\Delta K_{eff}$ | Effective stress intensity range, MPa$\sqrt{m}$ |
| $K_{OL}$ | Overload stress intensity, MPa$\sqrt{m}$ |
| $K_{res}$ | Stress intensity due to residual stress, MPa$\sqrt{m}$ |
| $m(a, x)$ | Weight function for evaluation of stress intensity |
| $n$ | Strain hardening exponent |
| $N$ | Number of cycles |
| $U$ | Closure value ($=\Delta K_{eff}/\Delta K$) |
| $\sigma$ | Nominal stress, MPa |
| $\Delta\sigma$ | Nominal stress range, MPa |
| $\sigma_{res}$ | Residual stress, MPa |
| $\sigma_y$ | Yield stress, MPa |
| $\sigma_{UTS}$ | Ultimate tensile stress, MPa |
| $\Delta\epsilon$ | Strain range |
| $x$ | Distance ahead of slit tip ($=a - a_0$), mm |

## INTRODUCTION

FATIGUE crack growth due to fully or partially tensile loadings has been well studied and documented. Empirical laws which successfully correlate growth rate with the stress intensity range, $\Delta K$, under different mean stresses, have been proposed. Traditionally, for partial tensile loadings, the negative portion of the applied stress intensity range is ignored; it is assumed that no crack growth occurs when a crack is closed. For fully compressive cycling, this approach predicts no fatigue damage. In practice, fatigue cracks can develop under compressive loading, for example cracks perpendicular to the direction of compressive loading in a coil spring, "shelling" in railway rails and cracks in the fillet joining the web and head of a rail[1]. Why do such cracks develop? It is argued that a tensile residual stress may exist in a region of compressive loading, where stress raisers or discontinuities exist. The extent of the tensile stress field depends on the extent of plastic yielding. A simple approach is that the crack grows to the boundary of the residual tensile field. This has been observed in laboratory tests[2–5] and in engineering components such as the coil spring mentioned above.

Several attempts have been made to model the residual tensile stress field and thereby predict the stress intensity range[3, 4] experienced by the crack tip.

The present study is directed towards finding the part of the load cycle during which the crack is open, quantified by $\Delta K_{eff}$. Crack closure is monitored using near tip strain gauges. Residual stresses are estimated and compared with a theoretical model. A refined residual stress model is used to predict crack growth rates.

Table 1. Composition and tensile properties of BS4360 Grade 50B structural steel

| Elemental composition (%) | | | | | |
|---|---|---|---|---|---|
| C | Mn | Si | P | S | Al |
| 0.14 | 1.27 | 0.41 | 0.017 | 0.004 | 0.073 |

| Properties* | | |
|---|---|---|
| Yield stress | Ultimate tensile stress | Elongation |
| 352 MPa | 519 MPa | 36 % |

* tensile properties relate to the roll direction

## EXPERIMENTAL

Specimens were made from BS4360 50B steel. The mechanical properties are given in Table 1, and the specimen geometry is shown in Fig. 1. The fine slits were cut using a jeweller's saw ($\sim 0.5$ mm wide) and sharpened with a razor blade. The specimens were stress-relieved in a muffle furnace at 650°C for one hour, followed by a slow furnace cool.

Tests were carried out in a Losenhausenwerk machine with the specimens fixed between a pair of compression platens.

An initial compressive cycle was applied to each specimen, Fig. 2. Deformation bands were observed near the slit tips, Fig. 3. The extent of these bands was different at each crack tip. This was due to slight machine misalignment.

The specimen was then removed from the testing machine and a strain gauge was bonded just behind one of the slit tips, see Fig. 1. This strain gauge was used for crack closure measurements.

Four different load sequences were employed for fatigue testing, Fig. 2. Crack lengths were measured with a travelling microscope. In order to be able to take readings without stopping the machine, a stroboscope was used to reduce apparent motion of the crack tip. Both test and stroboscope frequencies were set at 1000 cycles per minute. Minor variations in test frequency with respect to stroboscope frequency made it difficult to determine the exact location of the crack tip. This, together with the difficulty of locating the tip in a region of significant cyclic plasticity, led to a measurement uncertainty of $\pm 0.05$ mm. A crack was assumed to be arrested if no growth was detected after $\sim 10^6$ cycles.

The strain gauge and load cell bridge outputs were connected to an offset circuit [6] to enable a precise measurement of the crack closure load. A trace of load against offset-strain was displayed on an oscilloscope and was recorded photographically after each measurement of crack length was made.

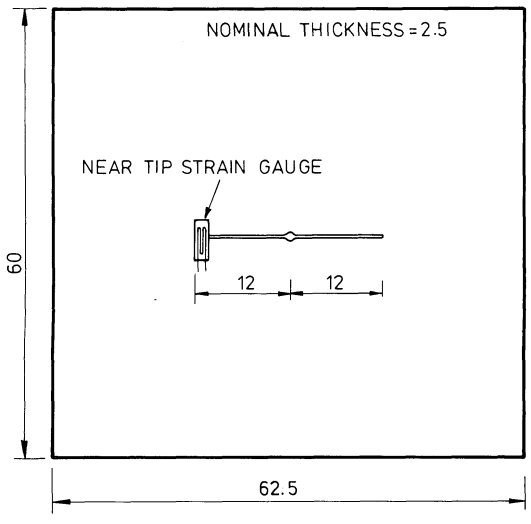


Fig. 1. Specimen geometry. All dimensions are in mm.

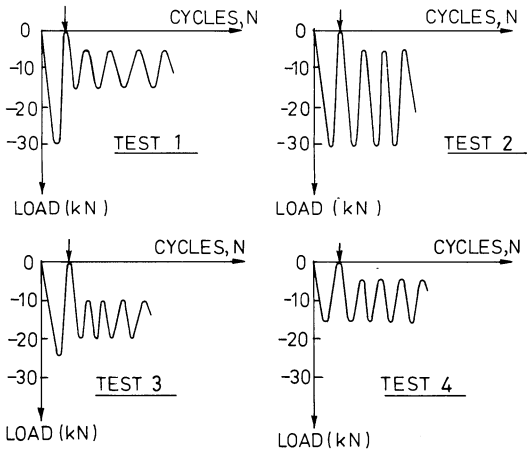


Fig. 2. Load histories employed. The arrow indicates the stage at which a strain gauge was bonded to the specimen.

## RESULTS

*Crack growth data*

No growth was observed for test 3 after $1.4 \times 10^6$ cycles. For the other tests, a small amount of crack growth occurred before arrest. Table 2 gives the final crack lengths as a percentage of the overload plastic zone sizes, calculated using Dugdale's strip yield model[7]. It was observed that the amount of growth depended both on the size of initial overload and the subsequent cyclic stress range.

Graphs of log (cracks length, a) vs log (cycles, N) were plotted, Fig. 4. A straight line could successfully be fitted to each set of data, in agreement with the results of Hubbard[2].

Growth rates were determined by drawing tangents to the curves of crack length versus number of cycles. Figure 5 shows the growth rates at different crack lengths for the three tests. The crack growth rate decreased steadily with increasing crack length.

The fraction of the applied load cycle for which the crack is open, $U$, may be deduced from the measured growth rates, as follows. The nominal stress intensity range, $\Delta K$, is deduced from the applied stress range, $\Delta\sigma$, using an equation given in Ref.[8]:

$$\Delta K = \Delta\sigma \cdot \sqrt{\pi a} \cdot \sqrt{\sec\left(\frac{\pi a}{2b}\right)} \tag{1}$$

The effective stress intensity range, $\Delta K_{\text{eff}}$, is related to crack growth rate, $da/dN$, in this material, by an expression given by Fleck[9]:

$$\frac{da}{dN} = 1.48 \times 10^{-8} (\Delta K_{eff})^{2.86} \text{ mm/cycles} \tag{2}$$

where $\Delta K_{\text{eff}}$ is given in units of MPa$\sqrt{\text{m}}$.

Table 2. Comparison of forward plastic zone size due to first load cycle and final crack length at surface of specimen

| | Test 1 | Test 2 | Test 3 | Test 4 |
|---|---|---|---|---|
| (1) Forward plastic zone size due to first load cycle* (mm) | 4.32 | 4.17 | 5.26 | 1.9 |
| (2) Crack growth increment at arrest (mm) | 1.26 | 2.48 | 0 | 0.68 |
| Ratio, (2)/(1) | 30% | 60% | 0% | 36% |

* Plastic zone size $= \frac{\pi}{8}\left(\frac{K_{max}}{\sigma_y}\right)^2$

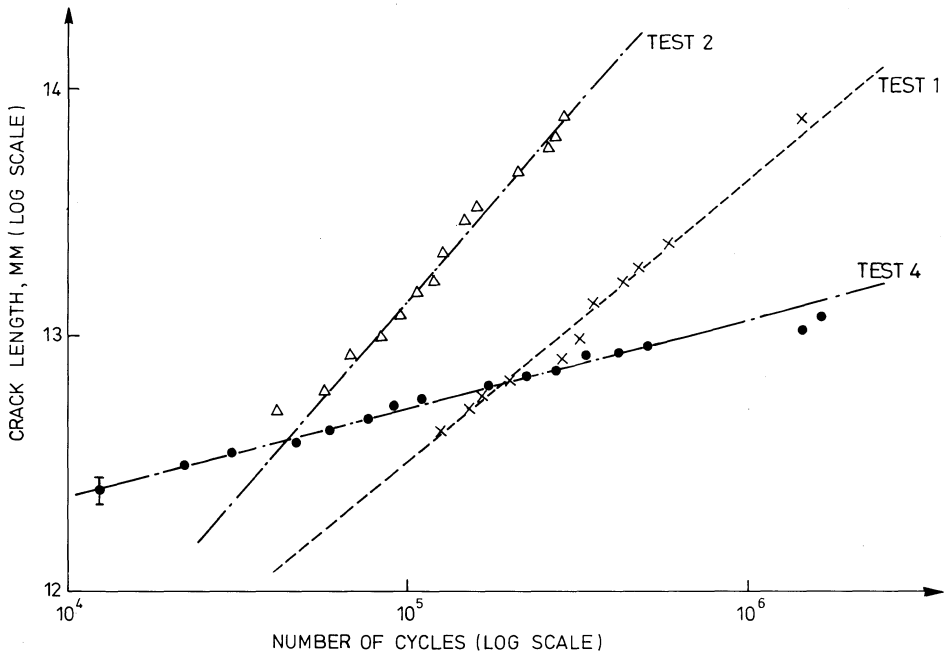


Fig. 4. Crack growth responses.

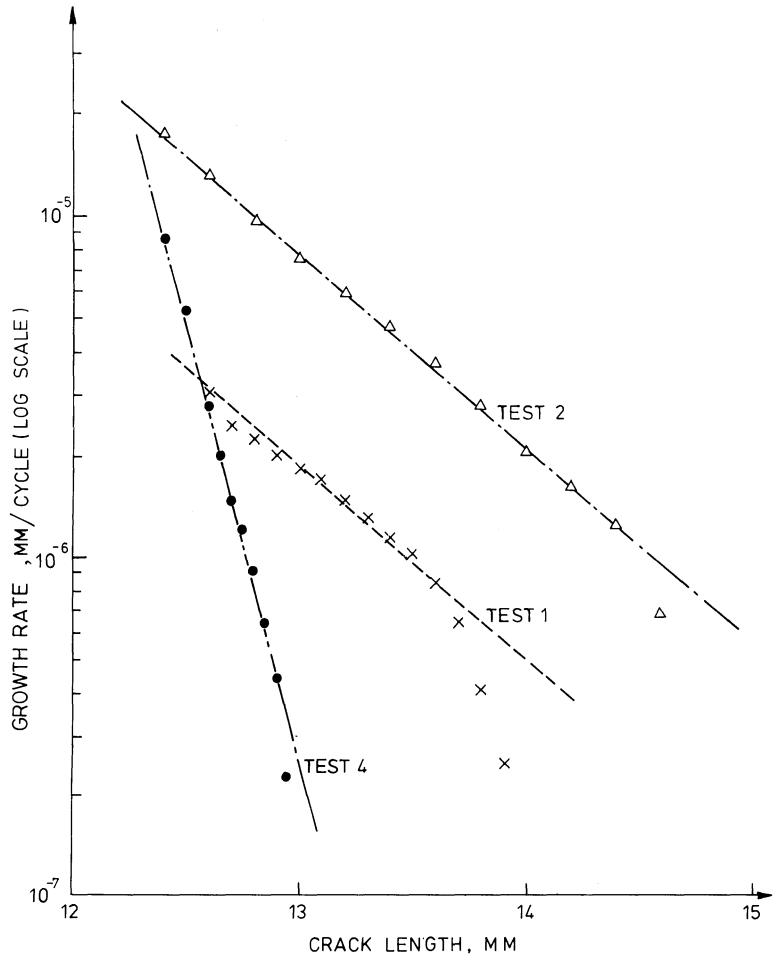


Fig. 5. Crack growth rate vs crack length for each test.

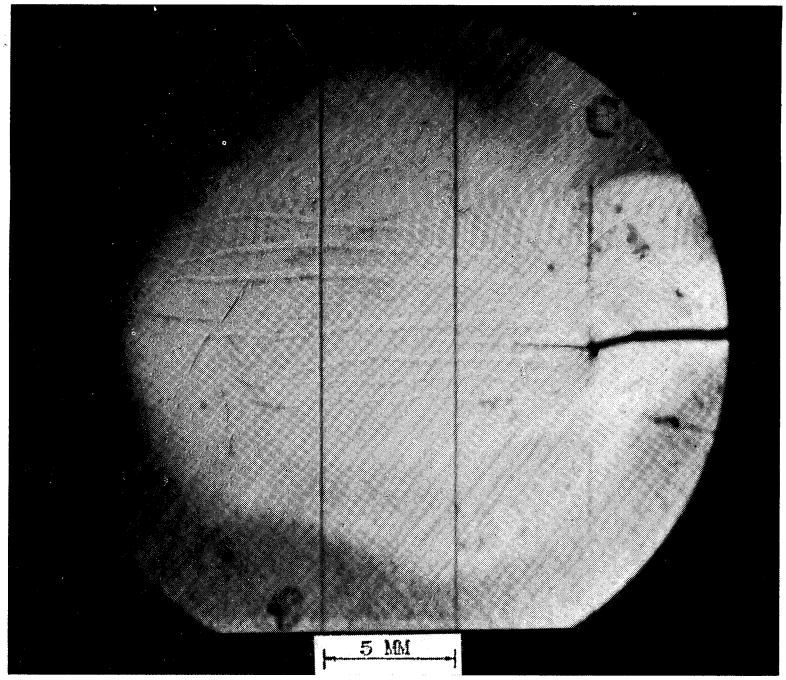


Fig. 3. Deformation bands near the slit tip, due to first load cycle.

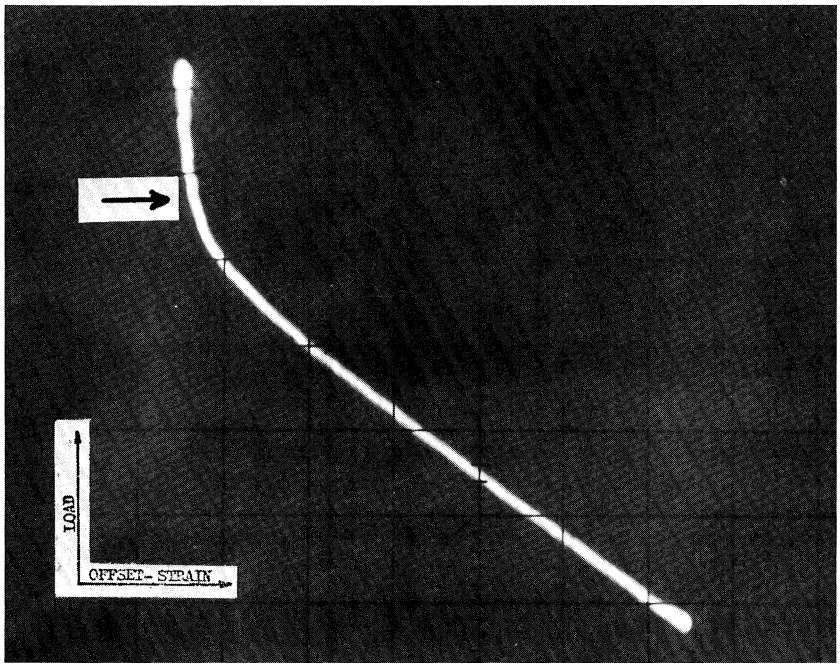


Fig. 6. Typical load offset-strain trace. Closure load is marked by an arrow.

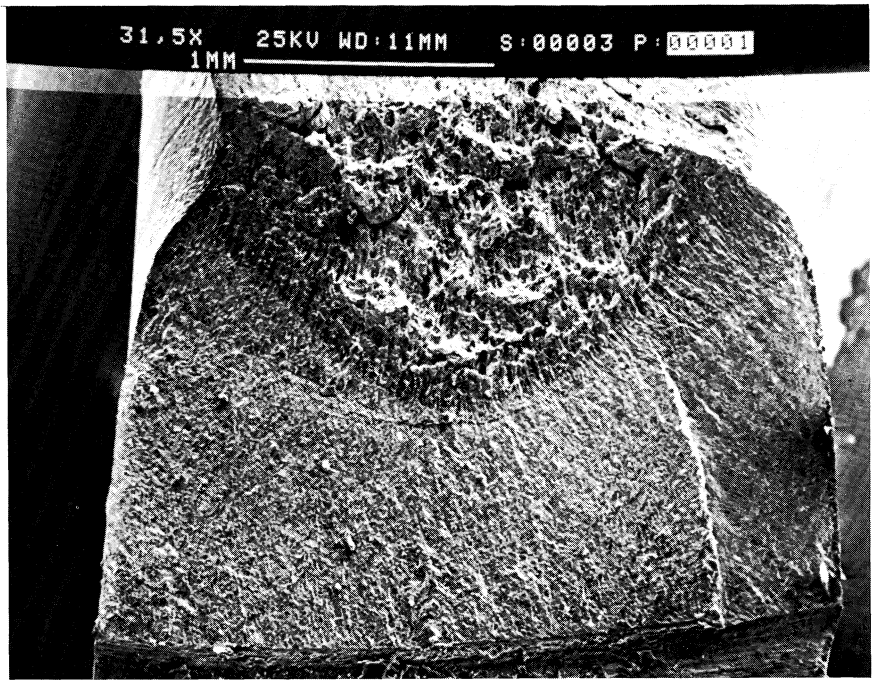


Fig. 8. Fatigue fracture surface. Test 2. Arrow shows direction of crack growth.

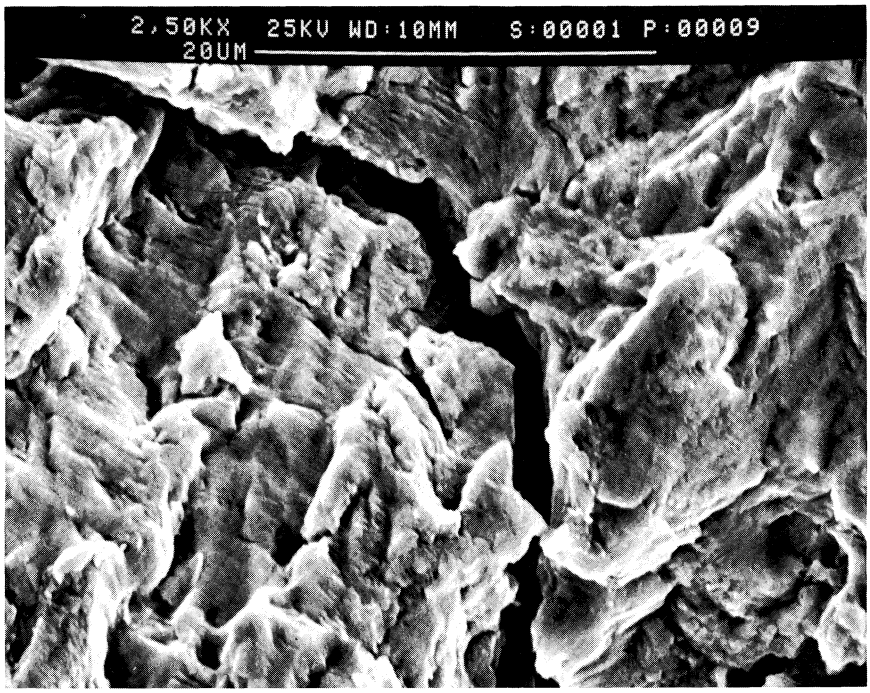


Fig. 9. Striations on fatigue fracture surface. Arrow shows direction of crack growth.

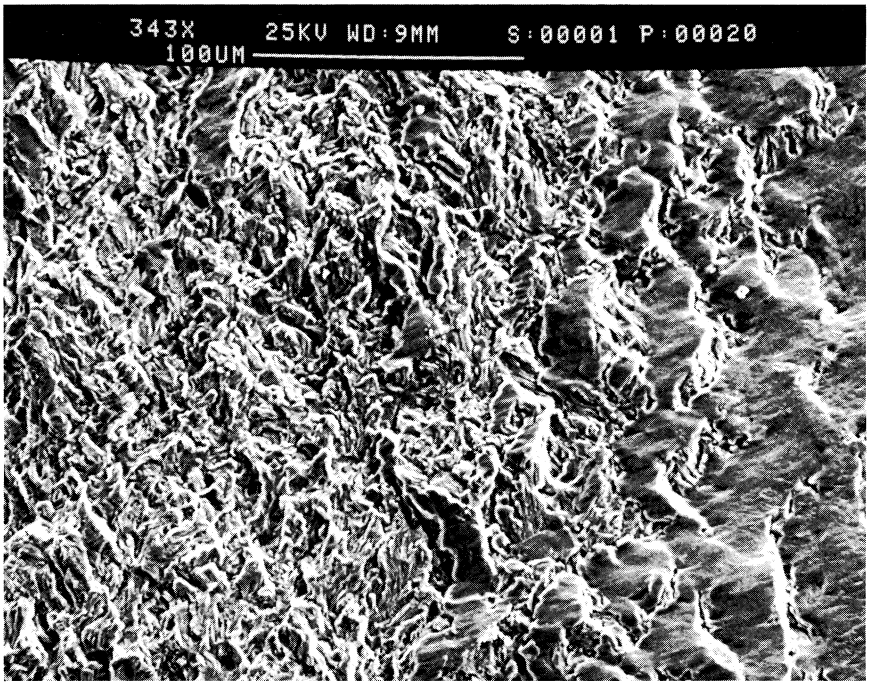


Fig. 10. Smearing of fatigue fracture surface. Arrow shows direction of crack growth.

We may then calculate, $U$, since $U = \Delta K_{\text{eff}}/\Delta K$.

$U$ values were also measured from the load offset-strain traces, Fig. 6. The load at which the vertical trace first becomes non-linear was used to define the closure load. Measured and inferred $U$ values show good agreement, see Fig. 7.

*Fractography*

The fracture surfaces of Specimen 2 were examined in a scanning electron microscope. It was observed that the crack length varied across the thickness of the specimen, being least at mid-thickness, Fig. 8. The ratio of maximum to minimum crack length measured from the starter slit was approx. 2.

This difference in crack length may be attributed to the difference in stress states along the crack front. At the surface, plane stress conditions prevail and a larger plastic zone is formed. At mid-thickness, plastic constraint is larger and so a smaller plastic zone is formed. The extent of residual tensile stress varies with the plastic zone size. Since residual tensile stress is required for crack growth, a difference in crack lengths through the thickness is expected.

Striations were observed on the fatigue fracture surface, as shown in Fig. 9, indicating tensile opening of the crack. However some randomly distributed smearing of the fracture surface was also apparent, Fig. 10, indicative of small areas of rubbing and/or sliding of the surfaces.

## PREDICTION OF RESIDUAL STRESSES NEAR THE CRACK TIP

Based on a modification of the results of Rice[10] and Majumdar *et al.*[11], Stouffer and Williams[12] described the stresses and strains normal to the crack plane and a distance $x$ ahead of the crack tip as:

$$\sigma\epsilon = \frac{K^2}{\pi(n+1)E(x+x_{ct})} \tag{3}$$

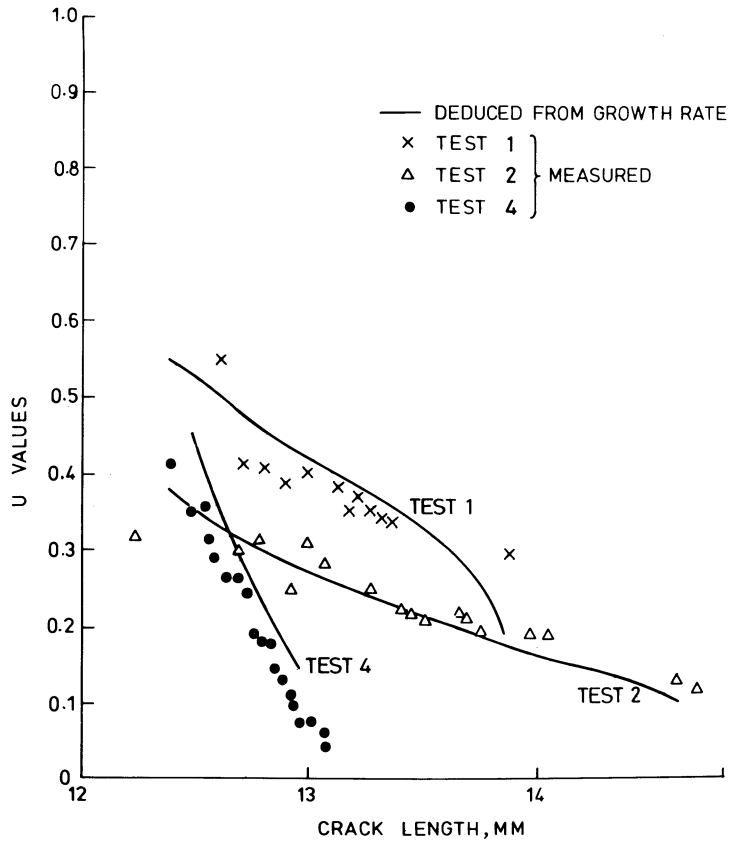


Fig. 7. Comparison of measured and inferred $U$ values.

where $x_{ct}$ = a constant obtained by putting $\Delta\sigma$ equal to the ultimate cyclic stress range, $\Delta\sigma_0$, at $x = 0$. we assume that eqn (3) also models the stress–strain state ahead of a sharp slit tip.

We approximate the stress–strain characteristic of the material using the Ramberg–Osgood relations:

$$\epsilon = \frac{\sigma}{E} \qquad \text{for } \epsilon < \frac{\sigma_y}{E}$$
$$\epsilon = \frac{\sigma}{E} + \left(\frac{\sigma}{A}\right)^{1/n} \qquad \text{for } \epsilon \geqslant \frac{\sigma_y}{E} \tag{4}$$

For unloading and subsequent cycling, we assume the material obeys Masing's postulate:

$$\Delta\epsilon = \frac{\Delta\sigma}{E} \qquad \text{for } \frac{\Delta\epsilon}{2} < \frac{\sigma_y}{E}$$
$$\frac{\Delta\epsilon}{2} = \frac{\Delta\epsilon}{2E} + \left(\frac{\Delta\sigma}{2A}\right)^{1/n} \qquad \text{for } \frac{\Delta\epsilon}{2} \geqslant \frac{\sigma_y}{E} \tag{5}$$

The stress distribution, $\sigma(x)$, on first loading is calculated from eqns (3) and (4). The change in stress distribution, $\Delta\sigma(x)$, due to unloading is calculated from equations (3) and (5). The residual stress distribution at zero load equals $\sigma(x) + \Delta\sigma(x)$

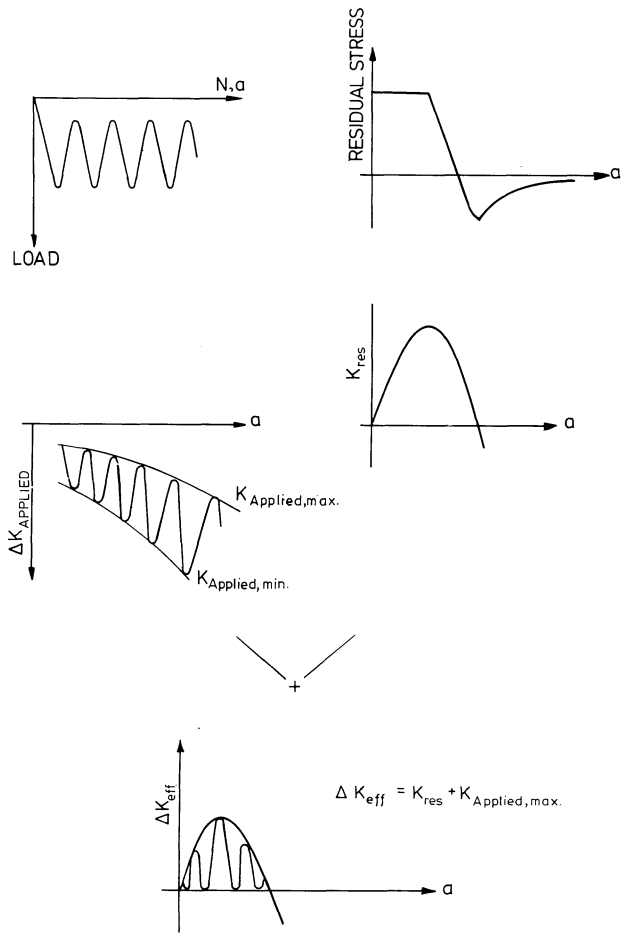


Fig. 11. Calculation of stress intensity factors using the superposition technique.

*Deduction of residual stress from measured growth rates*

The residual stress intensity factor, $K_{res}$, may be calculated from the residual stress profile, using Bueckner's principle[13, 14]:

$$K_{res}(a) = \int_{a_0}^{a} \sigma_{res}(x) m(a,x)\, dx \tag{6}$$

where $m(a, x)$ is the weight function.

We assume that the crack opens when applied and residual stress intensities sum to zero. Thus the effective stress intensity range, $\Delta K_{eff}$, becomes

$$\Delta K_{eff} = K_{res} + K_{applied,\ max.} \tag{7}$$

see Fig. 11.

We may reverse the above procedure. That is, after obtaining $\Delta K_{eff}$ from the growth rates, $K_{res}$ can be deduced from eqn (7) and $\sigma_{res}(x)$ from equation (6), see [15].

The residual stresses obtained in this way are greater than those given by eqns (3–5), see Fig. 12. If the constant $\pi$ in eqn (3) is replaced by $\pi/6$, then the new predictions of eqns (3–5) lie close to the residual stresses deduced from growth rates, except for small $x$, see Fig. 12. We attach no physical significance to the replacement of the constant $\pi$ in eqn (3) by $\pi/6$.

Figure 13 shows normalised residual stress, $\sigma_{res}/\sigma_y$, against the normalised distance, $x\sigma_y^2/K_{OL}^2$, for small $x$. Residual stresses deduced from Hubbard's compression tests on 7075–T6 aluminum alloy specimens[3] are included. The data fall in a scatter band given by:

$$\frac{\sigma_{res}}{\sigma_y} = B\left(\frac{K_{OL}^2}{x\sigma_y^2}\right)^{0.56} \tag{8}$$

where $4.6 < B < 8.0$. The centre of the band is given by $B = 6$. Equation (8) gives a $1/x^{0.56}$ dependence of $\sigma_{res}$ in contrast with the less steep gradient of $1/x^{n/n+1} (= 1/x^{0.17}$, for $n = 0.2$), suggested by Rice and Rosengren[16].

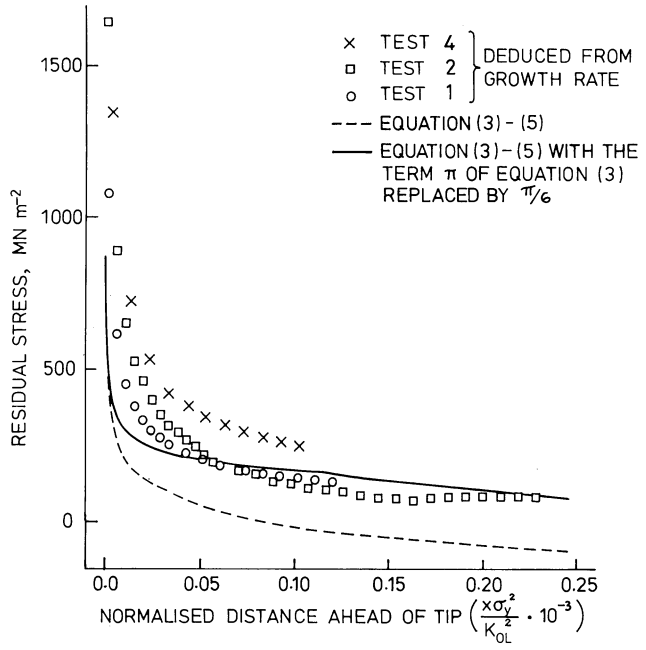


Fig. 12. Comparison of residual stress deduced from growth rates with residual stress predicted by eqns (3–5).

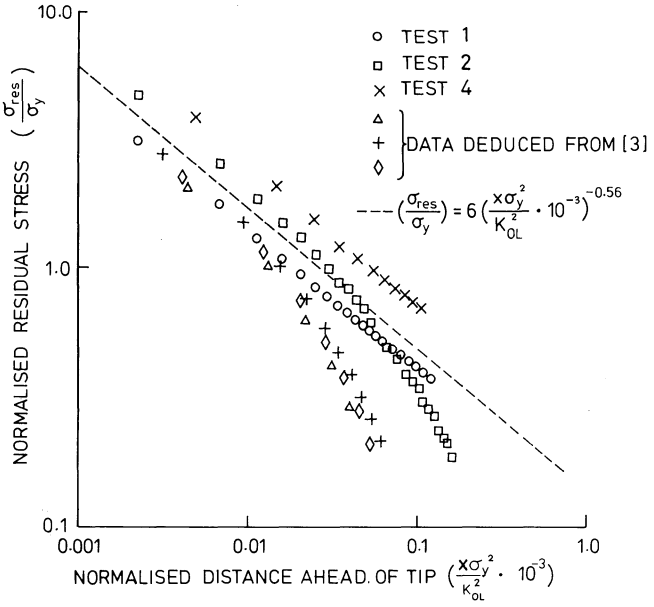


Fig. 13. Residual stresses deduced from growth rates. Results of present study, and Hubbard[3].

*Prediction of growth rates from residual stress models*

As illustrated schematically in Fig. 11, the effective stress intensity range $\Delta K_{eff}$, and hence crack growth rates $da/dN$ can be calculated from the residual stress distribution. Several stress distributions were employed and the predicted growth rates were compared with the experimental data.

The first profile used was the Williams–Stouffer model with the term $\pi$ replaced by $\pi/6$ (eqns 3–5). No growth was predicted near the slit tip as $\Delta K_{eff}$ was below the threshold value, Fig. 14. The growth rate then rose monotonically and became greater than the measured growth rate at some point near crack arrest. Obviously, the model fails.

The second profile used is eqn (8), with $B = 6$. Since eqn (8) describes the stresses in the vicinity of the slit tip, good agreement between predicted and measured growth rates was found in this region but not farther away from the slit tip, Fig. 14.

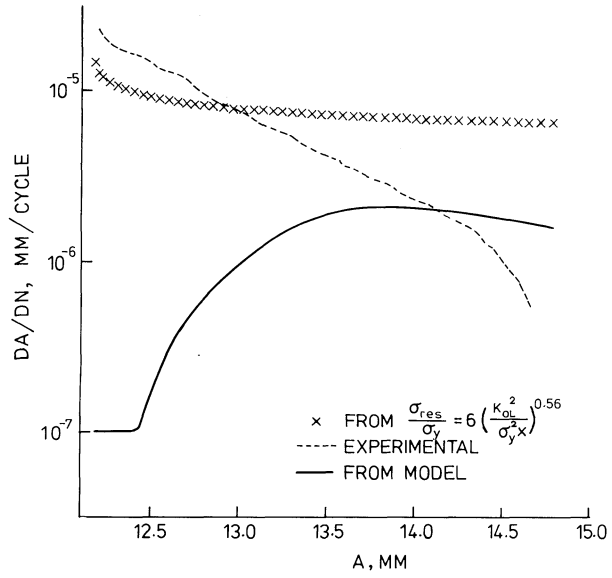


Fig. 14. Comparison of measured and predicted crack growth rates. Test 2.

Better agreement between predicted and measured growth rates could not be achieved for the following reasons:

1. Equation (8) failed to characterize the residual stress field near the location of crack arrest.
2. Equation (8) predicts infinite residual stress at the slit tip. In reality, residual stresses do not exceed the true stress at failure in a plain tensile specimen.
3. Any error in residual stress leads to a much larger error in the predicted growth rate, since growth rates approximately scale with the third power of $\Delta K_{\text{eff}}$.

## CONCLUSIONS

1. Even though the external loading may be compressive, fatigue cracks may grow due to the presence of residual tensile stress fields near stress concentrators.
2. Such fatigue crack growth rates may be correlated with the effective stress intensity range using the crack closure concept. As crack length increases, the fraction of the load cycle for which the crack is open decreases, and arrest eventually occurs.
3. The residual tensile stress, $\sigma_{\text{res}}$, near a crack-like stress concentrator may be approximated by a model similar to that of Stouffer and Williams, i.e. $\sigma\epsilon \propto 1/(x + \text{const.})$. This model fails close to the slit tip, where $\sigma_{\text{res}}$ scales with distance, $x$, from the slip tip as $\sigma_{\text{res}} \propto (1/x^{0.56})$.

*Acknowledgements*—One of the authors (CSS) is supported by a Research Scholarship from Corpus Christi College; another author (NAF) is funded by the Maudslay Research Fellowship at Pembroke College. The authors wish to thank Mr M. C. Smith for useful discussions, and British Gas for provision of test materials.

## REFERENCES

[1] J. O. Almen and P. H. Black, *Residual Stresses and Fatigue in Metals*. McGraw-Hill, New York (1963).
[2] T. L. Gerber and H. O. Fuchs, Analysis of non-propagating fatigue cracks in notched parts with compressive mean stress. *J. Mater.* **3**, 359–374 (1968).
[3] R. P. Hubbard, Crack growth under cyclic compression. *J. Basic Engng, Trans. ASME* **91**, 625–631 (1969).
[4] H. Saal, Fatigue crack growth in notched parts with compressive mean loads. *J. Basic Engng Trans. ASME* **94**, 243–247 (1972).
[5] C. N. Reid, K. Williams and R. Hermann, Fatigue in compression. *Fat. Engng Mat. Struct.* **1**, 267–270 (1979).
[6] N. A. Fleck, The use of compliance and electrical resistance techniques to characterize fatigue crack closure. *Tech. Rep. CUED/C/MATS/TR.* 89 Cambridge University, (1982).
[7] D. S. Dugdale, Yielding of steel sheets containing slits. *J. Mech. Phys. Solids* **8**, 100–104 (1960).
[8] H. Tada, P. Paris and G. Irwin, *The Stress Analysis of Crack Handbook*. Del Research Corporation (1973).
[9] N. A. Fleck, An investigation of fatigue crack closure, PhD. Thesis, Cambridge University, Cambridge (1983).
[10] J. R. Rice, Stress due to a sharp notch in a work hardening elastic–plastic material loaded in longitudinal shear. *J. Appl. Mech., Trans. ASME* **34**, 287–298 (1967).
[11] S. Majumdar and J. Morrow, Correlation between fatigue crack propagation and low cycle fatigue properties. *ASTM STP* **559**, 159–182 (1974).
[12] D. C. Stouffer and J. F. Williams, A model for fatigue crack growth with a variable stress intensity factor. *Engng Fracture Mech.* **11**, 523–536 (1979).
[13] H. F. Bueckner, A novel principle for the computation of stress intensity factors. Zeitschrift fur Angewandte Mathematik und Mechanik **50**, 529–546 (1970).
[14] D. V. Nelson, Effect of residual stress on fatigue crack propagation. *ASTM STP* **776**, 172–184 (1982).
[15] L. M. Delves and J. Walsh, *Numerical Solution of Integral Equations*. Clarendon Press, Oxford (1974).
[16] J. R. Rice and G. F. Rosengren, Plain strain deformation near a crack tip in a power-law hardening material. *J. Mech. Phys. Solids* **16**, 1–12 (1968).

(*Received* 22 *September* 1983)